

Magneto-responsive Smart Capsules Formed with Polyelectrolytes, Lipid Bilayers and Magnetic Nanoparticles

Kiyofumi Katagiri,* Masato Nakamura, and Kunihito Koumoto

Department of Applied Chemistry, Graduate School of Engineering, Nagoya University, Furo-cho, Chikusa-ku, Nagoya 464-8603, Japan

ABSTRACT Magneto-responsive smart capsules formed with polyelectrolytes, lipid bilayers and magnetic nanoparticles were fabricated by a colloid-templating technique. Melamine-formaldehyde core particles with polyelectrolyte multilayer shell were prepared by layer-by-layer assembly. Magnetite (Fe_3O_4) nanoparticles were selectively deposited on the capsular surface by aqueous solution deposition using Pd catalysts. Hollow capsules were obtained by the removal of the melamine formaldehyde core particles. Vibrating sample magnetometer (VSM) measurement of the capsules revealed the ferromagnetic behavior of deposited Fe_3O_4 nanoparticles. Alternating magnetic field irradiation generates heat in the capsular dispersion. Additional lipid bilayer coating was carried out on the obtained hollow capsules. Dye molecules were loaded by exploiting the temperature-dependence of the lipid membrane permeability. An encapsulated dye was released on-demand by irradiation with an alternating magnetic field, due to a phase transition in the lipid membrane, induced by heating of the magnetic nanoparticles. The magnetically induced release is attributed to the phase transition of the lipid membrane, caused by heat of Fe_3O_4 nanoparticles under magnetic stimuli, and not to rupture of the capsules.

KEYWORDS: organic–inorganic hybrid • drug delivery system • hollow capsule • lipid bilayer • layer-by-layer assembly

1. INTRODUCTION

Microcapsules have been widely investigated over the past few decades and have attracted great interest in the areas of drug delivery, agriculture, and the food and cosmetics industries (1). Key requirements of delivery vehicles in medical and pharmaceutical applications are (i) that they can be controllably loaded with active materials; (ii) that they have a long-term stability during storage; (iii) that they have a high loading capacity; (iv) that they transport their load specifically to the targeted site; and (v) that they release their load in a controlled manner. A versatile technique for preparation of microcapsules with control over their size, stability, loading, and release properties is layer-by-layer (LbL) assembly (2, 3) on colloid templates (4–6). This process involves the successive deposition of various materials, assembled alternately through complementary interactions (e.g., electrostatics, H-bonding, covalent bonding) onto colloidal particles, followed by particle removal. A number of “smart capsules” with stimuli-responsive behavior have been reported (7–11). Typically, the active material is entrapped within capsules and undergoes release in response to an environmental trigger such as a change in pH, temperature, ionic strength and/or enzyme concentration (12–17). One of the most successful approaches is the optically induced delivery system (7, 9, 18). Caruso et al. showed that gold nanoparticle-functionalized capsules loaded with lysozyme (7a) or FITC-dextran (7b)

could be optically addressed by irradiation with near-infrared light to trigger release of the encapsulated substances. We have recently reported tunable UV-responsive release capsules formed with a sol–gel-derived SiO_2 – TiO_2 layer on a polyelectrolyte multilayer shell (19). However, light-triggered systems have disadvantages for medical applications. Human tissues are not transparent to UV light and the latter is toxic to human tissues. In the case of near-infrared (NIR) light, most tissues show only weak light absorption. However, a short pulse NIR light laser with a certain intensity is required for NIR-triggered systems (7).

On the other hand, a magnetic field is a potential candidate as an external field for an on-demand release system. Human tissues are sufficiently transparent to magnetic fields and are not damaged by them. Therefore, they have already been employed in the medical field, including magnetic resonance imaging (MRI) contrast media (20), separation of biochemical products (21), gene manipulation and immunoassay (22), and magnetic hyperthermia therapy (23, 24). Magnetic nanoparticles can generate heat in an alternating magnetic field because of hysteresis loss and/or Néel relaxations. Therefore, magnetic nanoparticles have been used in hyperthermia treatment in an attempt to realize specific heating of tumors without damaging normal tissues. Several studies of microcapsules containing magnetic nanoparticles have been reported (25–28). Li et al. reported a pH responsive drug release of magnetic microcapsules (25). Lvov et al. reported that polyelectrolyte microcapsules embedded with Co/Au can be activated by using an external magnetic field to modulate its permeability (26). Recently, Chen and co-workers have achieved controlled rupture of microcapsules by a magnetic field (27). These reports employed

* To whom correspondence should be addressed. E-mail: katagiri@apchem.nagoya-u.ac.jp.

Received for review November 11, 2009 and accepted February 22, 2010

DOI: 10.1021/am900784a

© 2010 American Chemical Society

macromolecules, such as FITC-dextran, as release substances. In contrast to these studies, most drugs have relatively low molecular weights and there are considerable challenges in encapsulating and releasing low molecular weight molecules from microcapsules using magnetic fields. In addition, a system that allows controlled release without shell rupture is desirable because “switchable” release may be important in drug delivery.

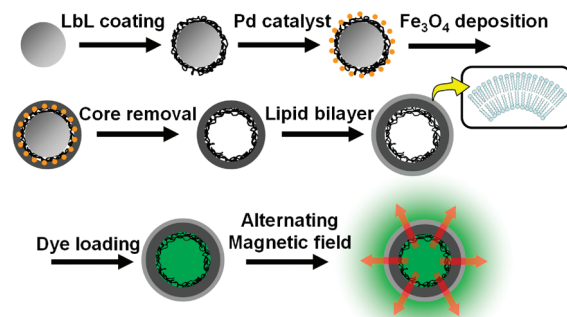
In this work, a magneto-responsive smart capsule was designed by a hybrid system using LbL-assembled polyelectrolytes, lipid bilayers, and magnetic nanoparticles. We show that these capsules are suitable for the stable encapsulation of low-molecular-weight compounds, which can be released upon irradiation with an alternating magnetic field. The stable encapsulation of small molecules in polyelectrolyte capsules is considerably more difficult than for macromolecules, because polyelectrolyte multilayers exhibit a high permeability to low-molecular-weight compounds (29). This permeability can be reduced by the deposition of lipid coatings on the capsules (30), thus offering a pathway for encapsulating small molecules. Membrane permeability of lipid bilayers changes with temperature through the “gel” to “liquid crystalline” phase transition. Meanwhile, magnetic nanoparticles can generate heat in an alternating magnetic field as described above. On the basis of these two phenomena, magneto-responsive microcapsules should be designable, functioning as follows. Irradiation with an alternating magnetic field will cause heating on the capsular shell of magnetic nanoparticles. A local temperature increase on the capsular shell will induce phase transition in the lipid membrane and encapsulated molecules should then be released from the interior of the capsules.

2. EXPERIMENTAL METHODS

2.1. Materials. Positively charged, weakly cross-linked melamine-formaldehyde (MF) particles (with diameter of 2.82 μm) were obtained from Microparticles GmbH, Berlin, Germany. Poly(allylamine hydrochloride) (PAH, $M_w = 70\,000\text{ g mol}^{-1}$) was purchased from Sigma-Aldrich. Poly(sodium *p*-styrenesulfonate) (PSS, $M_w = 70\,000\text{ g mol}^{-1}$) was obtained from Acros Organics. Iron(III) nitrate 9-hydrate, sodium chloride (NaCl), hydrochloric acid (HCl), and 2-(*N*-morpholino)ethanesulfonic acid 1-hydrate (MES) purchased from Kishida Chemical. Dimethylamine borane (DMAB), dioctadecyldimethylammonium chloride (DDAC), and Phenol red were obtained from Tokyo Chemical Industry. Sodium palladium(II)chloride (Na_2PdCl_4) was purchased from Mitsuwa Chemicals. Calcein was obtained from Dojindo Laboratories. All reagents were used as received without any further purification. The water used in all experiments was deionized by a Milli-Q system.

2.2. Preparation Procedure of Hybrid Capsules. Scheme 1 shows the procedure used for preparing magneto-responsive hybrid capsules by LbL assembly and aqueous phase deposition of magnetic nanoparticles. Polyelectrolyte shells were fabricated by the alternate assembly of poly(sodium 4-styrenesulfonate) (PSS) and poly(allylamine hydrochloride) (PAH) onto melamine formaldehyde (MF) particles. The core-shell particles, terminated by a PAH layer, were subsequently coated with Pd catalytic nanoparticles. Magnetite (Fe_3O_4) nanoparticles were directly deposited on Pd-catalyzed MF particles using an aqueous solution containing iron(III) nitrate. Hollow capsules were fabricated by removal of the MF particles by dissolution with

Scheme 1. Schematic Representation of Preparation Process and Release of Substances from Magneto-responsive Hybrid Capsules



HCl (5). The resulting capsules were additionally coated with a cationic lipid bilayer of dioctadecyldimethylammonium chloride (DDAC). Dye molecules were postloaded into the capsules by switching the lipid bilayer membrane permeability through the “gel” to “liquid crystalline” phase transition.

2.3. Polyelectrolyte Coating on Colloidal Particles. The polyelectrolyte multilayer-coated MF particles were prepared by LbL assembly. The positively charged MF particles were suspended in an aqueous solution of an anionic polyelectrolyte (i.e., PSS) (1 mg mL^{-1}) containing 0.5 M NaCl . The anionic polyelectrolyte was allowed to adsorb onto the colloids for 15 min. The dispersion was then centrifuged for 3 min at 2000 g followed by removal of the supernatant. The polyanion-coated particles were redispersed in deionized water by using a vortex mixer. Before the next coating step, the washing process (centrifugation, removal of supernatant, and redispersion) was repeated twice to remove any nonadsorbed polyelectrolyte. Deposition of a cationic polyelectrolyte (i.e., PAH) (1 mg mL^{-1} solution containing 0.5 M NaCl) on the polyanion-coated MF particles was carried out using the same method. PSS/PAH multilayers in the film was obtained by the alternate deposition onto the MF particles.

2.4. Preparation of Pd Catalysis. Hydrolyzed Pd colloids were prepared in the way described elsewhere (31, 32). A catalytic dispersion finally contained $\sim 0.35\text{ mM Na}_2\text{PdCl}_4$, $\sim 110\text{ mM NaCl}$, and $\sim 9\text{ mM MES}$. Polyelectrolyte-coated MF particles were dispersed in this Pd catalytic colloidal dispersion for 30 min at $25\text{ }^\circ\text{C}$. Negatively charged Pd catalytic colloids were adsorbed on the surface of polyelectrolyte-coated particles with positively charged PAH outmost layer mainly by electrostatic interaction. The washing process (centrifugation, removal of supernatant, and redispersion) was repeated twice to remove any nonadsorbed Pd nanoparticles.

2.5. Magnetite (Fe_3O_4) Deposition. Pd-catalyzed MF particles obtained as above were dispersed in an aqueous solution containing $2.5\text{ mM iron(III) nitrate}$ and 0.05 M DMAB for 30 min at $60\text{ }^\circ\text{C}$. DMAB was used to reduce nitrate ions, giving rise to OH^- ions and hence raising the solution pH to precipitate Fe_3O_4 . The deposition mechanism of Fe_3O_4 was described elsewhere (33, 34).

2.6. Preparation of Hollow Capsules. Core dissolution of MF was accomplished by exposure of Fe_3O_4 deposited particles (suspended in 0.5 mL water) to 0.1 M HCl aqueous solution (1 mL) for 30 min. The hollow capsules were centrifuged and redispersed in pure water. The MF cores were exposed to the HCl solution several times to remove MF oligomers remaining in the shell and the capsule interior. Finally, the hollow capsules were washed a further three times with deionized water.

2.7. Lipid Bilayer Coating and Dye Loading. Loading of dyes using for release measurements into hybrid hollow capsules formed with Fe_3O_4 and DDAC-bilayer were carried out in conjunction with lipid coating. The hollow capsules for lipid

coating were prepared from Fe_3O_4 -deposited MF particles further coated with $(\text{PSS}/\text{PAH})_4\text{PSS}$ via the same process described above. Multilamellar vesicles of DDAC were generated using a vortex mixer, and these liposomal dispersions were then ultrasonicated with a bath-type sonicator (70 W) for 2 h at a temperature above the phase-transition points of the DDAC to obtain small unilamellar vesicles (SUV). The concentration of lipid was fixed at 1.0 mM. DDAC SUVs were prepared using aqueous solutions of phenol red (1 mM) or calcein (1 mM). Deposition of the lipid bilayer on the PSS-terminated hollow capsules was performed by incubating for 2 h at 60 °C in a SUV dispersion of a DDAC (above the phase transition temperature of ca. 45 °C for the bilayer membrane of DDAC). The dispersion was then cooled to room temperature, and the capsules were collected by centrifugation. Further washing was carried out by three cycles of centrifugation/supernatant exchange (with deionized water)/redispersion. Lipid coating on hybrid hollow capsules formed with Fe_3O_4 was confirmed by fluorescent microscopy using fluorescence-probelipid (see the Supporting Information, Figure S1).

2.8. Transmission Electron Microscopy (TEM). Transmission electron microscopy (TEM) images and selected area electron diffraction (SAED) patterns were taken on a Hitachi H-800 microscope operated at 200 kV. TEM samples were prepared by depositing a droplet of the dispersion on a carbon-coated copper grid covered with polyvinylformal film and allowing them to air-dry overnight.

2.9. Magnetic Property Measurement. Magnetic properties were evaluated using a vibrating sample magnetometer (VSM; VSM-5-15, Toei Industry Co.) at room temperature.

2.10. Alternating Magnetic Field Irradiation. Alternating magnetic field irradiation for the hollow capsules was carried out with a high-frequency magnetic field generator (HI-HEATER 5010, Daiichi High Frequency). The frequency of alternating magnetic field was fixed to 360 kHz. The hollow capsule dispersion was putted in a 2 mL centrifuge tube. The tube was placed at the center of the coil of a high-frequency magnetic field generator. A photograph of the setup of the generator is given in the Supporting Information (Figure S2).

2.11. Fluorescence Microscopy. Fluorescence micrographs were taken with a Nikon Eclipse Ti-U microscope. Calcein was used as a fluorescent probe. The excitation wavelength was set at 450–490 nm. Fluorescence images were taken before and after alternating magnetic field irradiation at 360 kHz and 234 Oe for 30 min.

2.12. UV-Visible Spectroscopy. UV-visible spectroscopy was employed to investigate the release property of hybrid capsules. Hybrid capsules were dispersed in aqueous solution (pH 9.4) and irradiated with alternating magnetic field for certain periods of time. After irradiation, capsules were removed by centrifugation. Then the absorbance at 560 nm was measured by a UV-visible spectrophotometer for the obtained supernatants.

3. RESULTS AND DISCUSSION

Transmission electron microscopy (TEM) was used to follow the deposition of Fe_3O_4 on MF particles and to examine the morphology of the coated particles and hollow capsules obtained after removal of cores. In addition, the nanostructures of deposited Fe_3O_4 nanoparticles were also examined by TEM. Figure 1 shows TEM images of a core-shell particle formed with polyelectrolytes and Fe_3O_4 on a MF core (a) and a hollow capsule after removal of the MF core (b). A magnified TEM image and electron diffraction (ED) pattern of hollow capsules are also shown in Figure 1c,d, respectively. The bare MF particle was spherical and

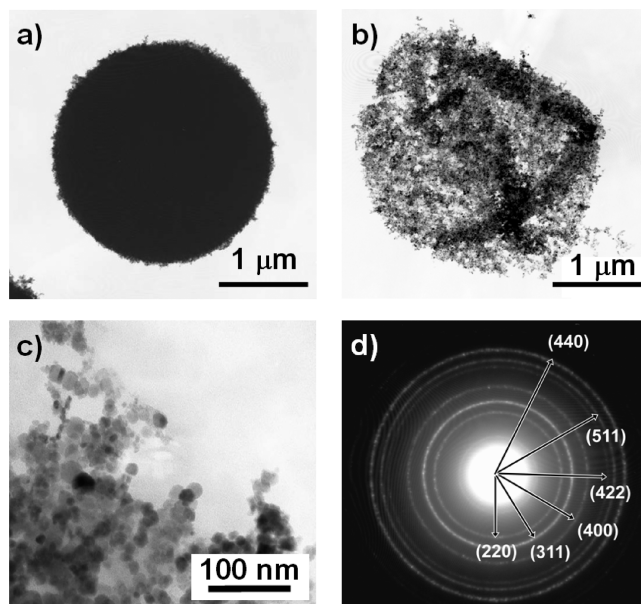


FIGURE 1. TEM images of (a) an Fe_3O_4 deposited MF particle coated with $(\text{PSS}/\text{PAH})_5/\text{Pd}$ and (b) a Fe_3O_4 /polyelectrolytes hollow capsule after removal of core. (c) Magnified image and (d) electron diffraction pattern of Fe_3O_4 /polyelectrolytes hollow capsules.

had a smooth surface. Deposition of five bilayers of PSS/PAH onto MF particle did not cause a noticeable change in the particle morphology (figure not shown). After deposition of Pd catalyst nanoparticles, the particle kept a smooth surface because the diameters of the nanoparticles were less than 30 nm and only small amounts of particles were deposited (figure not shown). Deposition of Fe_3O_4 is confirmed by Figure 1a. Fe_3O_4 was deposited rather uniformly on the surfaces of polyelectrolyte-coated MF particles. Figure 1b reveals formation of a hollow sphere via removal of the core MF template by HCl treatment. The size of a capsule was about 3 μm , reflecting that of the core MF particle. The numerous folds, creases and flattening of the capsules observed are attributed to capsule drying on a solid surface (35–37). This result indicates that deposited Fe_3O_4 was in the form of nanoparticles and not interconnected. The magnified image indicates that the deposited Fe_3O_4 nanoparticles had an average diameter of ca. 13 nm (Figure 1c). The ring patterns in the ED image shown in Figure 1d are assignable to the crystal faces of Fe_3O_4 , 220, 311, 400, 422, 511, and 440. This ED pattern indicates that the deposits on the core-shell particle were randomly oriented Fe_3O_4 nanocrystals. X-ray diffraction patterns of hollow capsules also revealed that Fe_3O_4 was deposited as nanocrystalline particles (see the Supporting Information, Figure S3). According to Scherrer's equation, the size of deposited Fe_3O_4 crystallite was evaluated as ca. 12 nm. This value corresponds well with that found in the magnified TEM image (Figure 1c).

The room-temperature hysteresis loop of the hollow capsules formed with Fe_3O_4 was measured using a vibrating sample magnetometer (VSM). The magnetization curves, as shown in Figure 2, display relatively high saturation magnetization. The magnetic saturation value was 78.6 emu/g, close to the theoretical value of 92 emu/g. The observed

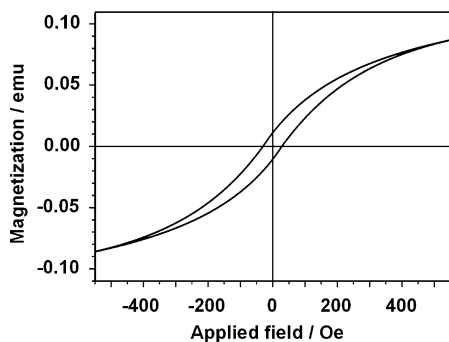


FIGURE 2. Vibrating sample magnetometer (VSM) measurement of the Fe_3O_4 /polyelectrolytes hollow capsules at room temperature.

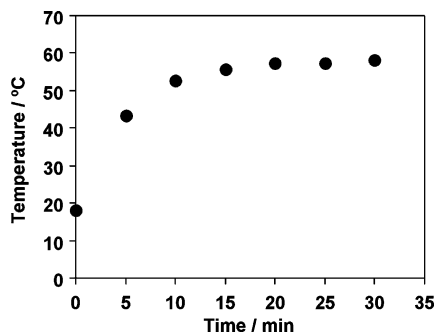


FIGURE 3. Temperature profile of the aqueous dispersion of Fe_3O_4 /polyelectrolytes hollow capsules as a function of irradiation time of alternating magnetic field at 360 kHz and 234 Oe.

values are within the range reported in the literature (38, 39). The reduced saturation magnetization of the capsules is probably due to the presence of organic substances, including polyelectrolytes, in the capsules. The hysteresis curve observed in the VSM measurement of the capsules produced by the aqueous solution process reveals the ferromagnetic behavior of deposited Fe_3O_4 nanoparticles. The microcapsules containing Fe_3O_4 display a satisfactorily high coercivity of 48.7 Oe at room temperature. These results indicate that the obtained microcapsules have a good ability to generate heat induced by alternating magnetic field irradiation.

Our strategy for the on-demand release function of microcapsules comprises heating the Fe_3O_4 nanoparticles by irradiation with an alternating magnetic field, causing changes in the permeability of lipid bilayer membrane by phase transition behavior. Therefore, temperature increases by heating of Fe_3O_4 nanoparticles have to reach beyond the phase transition temperature of the DDAC bilayer membrane, i.e., ca. 45 °C (40). We investigated whether an alternating magnetic field irradiation would generate enough heat in the capsular dispersion. A 5 mL capsular dispersion with a concentration of 5.5×10^8 capsules/mL was used for the measurement. The alternating magnetic field irradiation was carried out at 360 kHz and 234 Oe. The temperature of the dispersion rose significantly, reaching 58 °C, which is high enough to induce the phase transition of DDAC bilayer membrane (Figure 3).

The release behavior of the hybrid capsules formed with Fe_3O_4 nanoparticles and the lipid bilayer was initially investigated by fluorescence microscopy. Calcein was employed as a probe molecule because it is a convenient model for

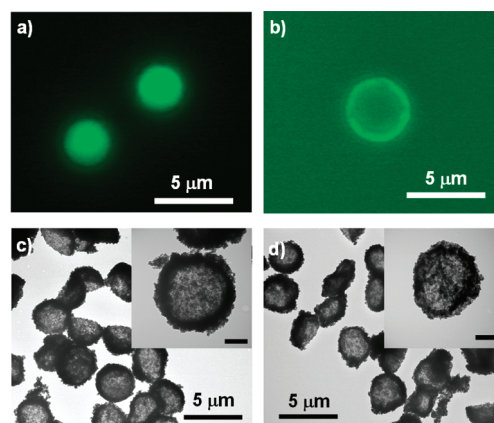


FIGURE 4. (a, b) Fluorescence microscope and (c, d) TEM images of hybrid capsules formed with polyelectrolytes, Fe_3O_4 nanoparticles and a DDAC bilayer membrane loaded with calcein (a, c) before and (b, d) after alternating magnetic field irradiation at 360 kHz and 234 Oe for 30 min. The scale bars in insets are 1 μm .

low molecular weight biomaterials, such as drugs. Images a and b in Figure 4 show fluorescence microscope images of the hybrid capsules formed with polyelectrolytes, Fe_3O_4 nanoparticles and a DDAC bilayer membrane loaded with calcein. Before alternating magnetic field irradiation, green fluorescence was observed only on the inside of capsules (Figure 4a), indicating that calcein was stably enclosed within the DDAC bilayer without a sign of leakage or release. In contrast, fluorescence was observed both inside and outside of the capsules after alternating magnetic field irradiation at 360 kHz and 234 Oe for 30 min (Figure 4b). This result indicates that the calcein was effectively released from the capsule under magnetic stimuli. A previous report by Chen et al. also showed release behavior of capsules under magnetic stimuli (27). They employed a macromolecular model, FITC-dextran, as the encapsulated substance. We show here loading and release of a low-molecular-weight substance, which is important because most drugs are not macromolecules. Usually, a polyelectrolyte multilayer shell has a high permeability for low-molecular-weight substances. Therefore, the lipid bilayer membrane plays an important role in the control of entrapment and release behavior of the hybrid capsules. In addition, the release from Chen et al.'s capsules was induced by rupture of the capsules, led by surface cracks after magnetic field irradiation. In contrast, it appears that no capsular rupture occurred in our capsules, judging from the fluorescence microscope images. TEM was used to confirm whether the alternating magnetic field irradiation caused rupture of capsules (Figure 4c,d). These images show almost the same capsule morphology before and after irradiation, confirming the absence of rupture. This indicates that the release from capsules was induced by the phase transition of the DDAC bilayer membrane, not by the rupture of capsular shells. Therefore, a switchable release system can be expected because the release of the encapsulated substance may be stopped by cessation of the alternating magnetic field irradiation.

We next quantitatively examined the release behavior of encapsulated substances. Phenol red was selected for use in these experiments since it has been widely examined in

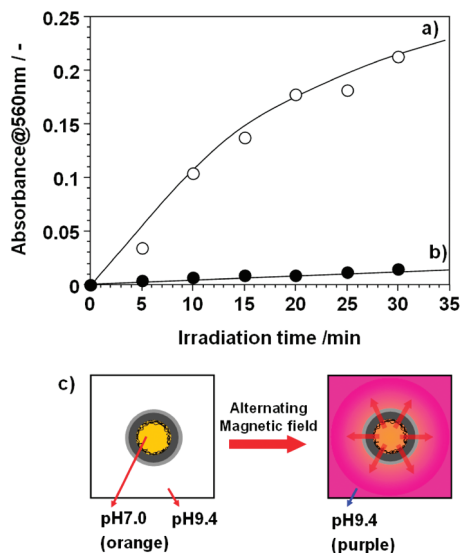


FIGURE 5. (a) Release of phenol red from the hybrid capsules, monitored by changes in dye absorbance at 560 nm as a function of irradiation time of alternating magnetic field (360 kHz and 234 Oe). (b) A control experiment was carried out by experiment without alternating magnetic field irradiation. (c) Schematic illustration of color change of the dispersion containing phenol red loaded capsules by magnetic field irradiation.

release studies from colloidal materials, including liposomes. Phenol red can act as an indicator, changing color at different pH values (19, 41). The dye was encapsulated in the internal aqueous phase of the lipid-coated capsules at pH 7.0 and above the phase-transition temperature of the lipid membrane. The molecular permeability of the membrane is high under this condition. After being cooled to 20 °C, the dye was sealed into the capsules because of the reduced permeability. The external aqueous phase was altered to pH 9.4. When the dye was released to the phase outside the capsules, the color changed to purple. Therefore, the release behavior could be detected by an increase in absorbance at 560 nm (the maximum absorbance of phenol red at pH 9.4). Figure 5 shows the changes in absorbance (560 nm) with time of exposure to the alternating magnetic field. A control experiment was carried out in the absence of the alternating magnetic field. The plots in Figure 5 are directly comparable because the same amount of encapsulated dye was used in each experiment. The hybrid capsules retained the dye, with no dye release observed over a period of 24 h at 10 °C. When the hybrid capsules formed with polyelectrolytes, Fe₃O₄ nanoparticles and a DDAC bilayer were irradiated with an alternating magnetic field, dye was released (Figure 5a). In contrast, there was a negligible increase in the absorbance after 30 min for capsules without the alternating magnetic field (Figure 5b), indicating virtually no dye release. In addition, almost no dye release was confirmed when the hollow capsules formed without Fe₃O₄ nanoparticles were irradiated with an alternating magnetic field (see the Supporting Information, Figure S4). These results indicate that the presence of Fe₃O₄ nanoparticles in the capsule shells induces phase transition in the DDAC by heat in the presence of an alternating magnetic field, causing dye release. The DDAC membrane and Fe₃O₄ nanoparticles were codepos-

ited on the surface of capsules. Therefore, the local heating of Fe₃O₄ nanoparticles on the capsular shell should be enough to trigger the dye release. It seems that the changes of bulk temperature of dispersion and the local temperature of capsular shell upon magnetic field irradiation have different trends. It should be the reason why the dye-release trend (Figure 5a) is different from that of the temperature profile (Figure 3).

4. CONCLUSIONS

Magneto-responsive microcapsules, comprising polyelectrolyte multilayers, lipid bilayers, and Fe₃O₄ nanoparticles, were prepared via the colloid-templating technique. It was shown that low-molecular-weight substances can be loaded into the capsules by exploiting the temperature-dependence of the lipid bilayer permeability. Encapsulated dyes can be released on-demand by alternating magnetic field irradiation. The magnetically induced release is attributed to the phase transition of the lipid membrane, caused by heat of Fe₃O₄ nanoparticles under magnetic stimuli, not to rupture of the capsules. In addition, hollow capsule prepared by the LbL process have the ability to encapsulate various kinds of substances (42). Therefore, such magneto-responsive capsules are strong candidates for drug delivery vehicles because the capsules can be magnetically guided to the target disease area (43) and tracked by MRI (20).

Acknowledgment. This work was supported by the Ministry of Education, Culture, Sports, Science and Technology (MEXT) of Japan (Grant-in-Aid for Young Scientists (A), 20686046, 2008–2009). The authors deeply appreciate the kind help for alternating magnetic field irradiation by Prof. Hiroyuki Honda and Dr. Ryuji Kato (Nagoya University). The authors thank Prof. Yoshinobu Baba and Dr. Noritada Kaji (Nagoya University) for assistance with fluorescence microscopy measurements. The authors also thank Prof. Toshinobu Yogo and Prof. Wataru Sakamoto (Nagoya University) for assistance with VSM measurements.

Supporting Information Available: Fluorescence microscope images of hybrid capsules, photograph of the setup of a high-frequency magnetic field generator, XRD pattern of hollow capsules, and control experiment of release property of capsule upon magnetic field irradiation (PDF). This material is available free of charge via the Internet at <http://pubs.acs.org>.

REFERENCES AND NOTES

- Lim, F. *Biomedical Applications of Microencapsulation*; CRC Press: Boca Raton, FL, 1984.
- (a) Decher, G.; Hong, J.-D. *Ber. Bunsen-Ges. Phys. Chem.* **1991**, *95*, 1430–1434. (b) Decher, G. Layered Nanoarchitectures via Directed Assembly of Anionic and Cationic Molecules. In *Comprehensive Supramolecular Chemistry*; SauvageJ.-P., Hosseini, M. W., Eds.; Pergamon Press: Oxford, U.K., 1996; Vol. 9, p 507.
- (a) Ariga, K.; Hill, J. P.; Ji, Q. *Phys. Chem. Chem. Phys.* **2007**, *9*, 2319–2340. (b) Ariga, K.; Hill, J. P.; Lee, M. V.; Vinu, A.; Charvet, R.; Acharya, S. *Sci. Technol. Adv. Mater.* **2008**, *9*, 01410.
- (a) Peyratout, C. S.; Dähne, L. *Angew. Chem., Int. Ed.* **2004**, *43*, 3762–3783. (b) De Geest, B. G.; Sanders, N. N.; Sukhorukov, G. B.; Demeester, J.; De Smedt, S. C. *Chem. Soc. Rev.* **2007**, *36*, 636–649. (c) Bédard, M. F.; De Geest, B. G.; Skirtach, A. G.; Möhwald, H.; Sukhorukov, G. B. *Adv. Colloid Interface Sci.* **2009**, doi: 10.1016/j.cis.2009.07.007.

- (5) Caruso, F. Ed., *Colloids and Colloid Assemblies*; Wiley-VCH: Weinheim, Germany, 2003.
- (6) Quinn, J. F.; Johnston, A. P. R.; Such, G. K.; Zelikin, A. N.; Caruso, F. *Chem. Soc. Rev.* **2007**, *36*, 707–718. (b) Zelikin, A. N.; Becker, A. L.; Johnston, A. P. R.; Wark, K. L.; Turatti, F.; Caruso, F. *ACS Nano* **2007**, *1*, 63–69.
- (7) (a) Radt, B.; Smith, T. A.; Caruso, F. *Adv. Mater.* **2004**, *16*, 2184–2189. (b) Angelatos, A. S.; Radt, B.; Caruso, F. *J. Phys. Chem. B* **2005**, *109*, 3071–3076. (c) Angelatos, A. S.; Katagiri, K.; Caruso, F. *Soft Matter* **2006**, *2*, 18–23. (d) Wang, Y.; Angelatos, A. S.; Caruso, F. *Chem. Mater.* **2008**, *20*, 848–858.
- (8) (a) Skirtach, A. G.; Antipov, A. A.; Shchukin, D. G.; Sukhorukov, G. B. *Langmuir* **2004**, *20*, 6988–6992. (b) Skirtach, A. G.; Javier, M. A.; Kreft, O.; Köhler, K.; Alberola, A. P.; Möhwald, H.; Parak, W. J.; Sukhorukov, G. B. *Angew. Chem., Int. Ed.* **2006**, *45*, 4612–4617.
- (9) Tao, X.; Li, J.; Möhwald, H. *Chem.—Eur. J.* **2004**, *10*, 3397–3403.
- (10) Zelikin, A. N.; Quinn, J. F.; Caruso, F. *Biomacromolecules* **2006**, *7*, 27–30.
- (11) Such, G. K.; Tjipto, E.; Postma, A.; Johnston, A. P. R.; Caruso, F. *Nano Lett.* **2007**, *7*, 1706–1710.
- (12) Tong, W.; Gao, C.; Möhwald, H. *Macromolecules* **2006**, *39*, 335–340.
- (13) Li, M. H.; Keller, P. *Soft Matter* **2009**, *5*, 927–937.
- (14) Akamatsu, K.; Yamaguchi, T. *Ind. Eng. Chem. Res.* **2007**, *46*, 124–130.
- (15) Köhler, K.; Möhwald, H.; Sukhorukov, G. B. *J. Phys. Chem. B* **2006**, *110*, 24002–24010.
- (16) Antipov, A. A.; Sukhorukov, G. B.; Möhwald, H. *Langmuir* **2003**, *19*, 2444–2448.
- (17) Sukhishvili, S. S. *Curr. Opin. Colloid Interface Sci.* **2005**, *10*, 37–44.
- (18) Yuan, X.; Fischer, K.; Schärtl, W. *Langmuir* **2005**, *21*, 9374–9380.
- (19) Katagiri, K.; Koumoto, K.; Iseya, S.; Sakai, M.; Matsuda, A.; Caruso, F. *Chem. Mater.* **2009**, *21*, 195–197.
- (20) Billotey, C.; Wilhelm, C.; Devaud, M.; Bacri, J. C.; Bittoun, J.; Gazeau, F. *Magn. Reson. Med.* **2003**, *49*, 646–654.
- (21) Ugelstad, J.; Berge, A.; Ellingsen, T.; Schmid, R.; Nilsen, T. N.; Mørk, P. C.; Stenstad, P.; Hornes, E.; Olsvik, Ø. *Prog. Polym. Sci.* **1992**, *17*, 87–161.
- (22) Nakayama, H.; Arakaki, A.; Maruyama, K.; Takeyama, H.; Matsunaga, T. *Biotechnol. Bioeng.* **2003**, *84*, 96–102.
- (23) Jordan, A.; Wust, P.; Föhling, H.; John, W.; Hinz, A.; Felix, R. *Int. J. Hyperthermia* **1993**, *9*, 51–68.
- (24) Ito, A.; Fujioka, M.; Yoshida, T.; Wakamatsu, K.; Ito, S.; Yamashita, T.; Jimbow, K.; Honda, H. *Cancer Sci.* **2007**, *98*, 424–430.
- (25) Li, L. L.; Chen, D.; Ding, M. H.; Tang, F. Q.; Meng, X. W.; Ren, J.; Zhang, L. *Acta Phys. Chim. Sin.* **2007**, *23*, 1969–1973.
- (26) Lu, Z.; Prouty, M. D.; Guo, Z.; Golub, V. O.; Kumar, C. S. S. R.; Lvov, Y. M. *Langmuir* **2005**, *21*, 2042–2050.
- (27) Hu, S. H.; Tsai, C. H.; Liao, C. F.; Liu, D. M.; Chen, S. Y. *Langmuir* **2008**, *24*, 11811–11818.
- (28) Lee, S. H.; Song, Y.; Hoseini, I. D.; Liddell, C. M. *J. Mater. Chem.* **2009**, *19*, 350–355.
- (29) Sukhorukov, G.; Brumen, M.; Donath, E.; Möhwald, H. *J. Phys. Chem. B* **1999**, *103*, 6434–6440.
- (30) Moya, S.; Donath, E.; Sukhorukov, G. B.; Auch, M.; Baumler, H.; Lichtenfeld, H.; Möhwald, H. *Macromolecules* **2000**, *33*, 4538–4544.
- (31) Brandow, S. L.; Dressick, W. J.; Marrian, C. R. K.; Chow, G. M.; Calvert, J. M. *J. Electrochem. Soc.* **1995**, *142*, 2233.
- (32) Dressick, W. J.; Dulcey, C. S.; Georger, J. H.; Calabrese, G. S.; Calvert, J. M. *J. Electrochem. Soc.* **1994**, *141*, 210.
- (33) Nakanishi, T.; Masuda, Y.; Koumoto, K. *Chem. Mater.* **2004**, *16*, 3484.
- (34) Izaki, M.; Shinoura, O. *Adv. Mater.* **2001**, *13*, 142.
- (35) Caruso, F.; Caruso, R. A.; Möhwald, H. *Science* **1998**, *13*, 1111–1114.
- (36) Donath, E.; Sukhorukov, G. B.; Caruso, F.; Davis, S. A.; Möhwald, H. *Angew. Chem., Int. Ed.* **1998**, *37*, 2202–2205.
- (37) Katagiri, K.; Matsuda, A.; Caruso, F. *Macromolecules* **2006**, *39*, 8067–8074.
- (38) Chikazumi, S. *Physics of Ferromagnetism*, 2nd ed.; Oxford University Press: Oxford, U.K., 1997.
- (39) Lee, Y.; Lee, J.; Bae, C. J.; Park, J. G.; Noh, H. J.; Park, J. H.; Hyeon, T. *Adv. Funct. Mater.* **2005**, *15*, 503–509.
- (40) Kunitake, T. *Angew. Chem., Int. Ed.* **1992**, *31*, 709–726.
- (41) Braganza, L. F.; Blott, B. H.; Coe, T. J.; Melville, D. *Biochim. Biophys. Acta* **1983**, *731*, 137–144.
- (42) Balabushevich, N. G.; Tiourina, O. P.; Volodkin, D. V.; Larionova, N. I.; Sukhorukov, G. B. *Biomacromolecules* **2003**, *4*, 1191–1197.
- (43) Patil, G. V. *Drug Dev. Res.* **2003**, *58*, 219–247.

AM900784A